Optimization of oil production through ex-situ catalytic pyrolysis of waste polyethylene with activated carbon

Ruming Pan, Marcio Ferreira Martins, Gerald Debenest

Optimization of oil production through ex-situ catalytic pyrolysis of waste polyethylene with activated carbon

Ruming Pan[a], Marcio Ferreira Martins[b], Gérald Debenest[a,*]

[a]Institut de Mécanique des Fluides de Toulouse (IMFT) - Université de Toulouse, CNRS-INPT-UPS, Toulouse, 31400, France

[b]Laboratory of Combustion and Combustible Matter (LCC), PPGEM, Federal University of Espírito Santo, Vitória, 29075-910, Brazil

Abstract: This study studied the ex-situ catalytic pyrolysis of waste polyethylene (WPE) with activated carbon (AC). It was found that the operating parameters and AC/WPE mass ratio had complex interactions on the WPE-AC catalytic pyrolysis oil and gas yields. A hybrid method of artificial neural network (ANN) coupled with genetic algorithm (GA) was used to establish the mathematical expressions of oil and gas yields under different conditions and optimize the conditions to obtain the highest oil yield. The R^2 values and the average absolute relative errors between the experimental and the ANN predicted values were 0.9992 and 0.60 %, and 0.9830 and 5.01 % in the training and the testing tests, respectively. The optimal oil production calculated by ANN-GA was 69.16 wt% under 479 °C, the AC/WPE mass ratio of 1, and 10 mL/min. The experimental oil yield was 69.63 wt% under the optimal parameters, which was close to the predicted value of ANN-GA. The WPE-AC catalytic pyrolysis oils

under different conditions were characterized by the Fourier-transform infrared spectroscopy

(FTIR) and the gas chromatography/mass spectrometry (GC/MS). The types of oil's functional groups did not change with different operating parameters and AC/WPE mass ratios. The oils were composed of alkenes, naphthenes, alkanes, and aromatic hydrocarbons ranging from C8 to C33. The operating parameters and AC/WPE mass ratio affected the oil fractions to a great extent.

Keywords: *Waste polyethylene; Ex-situ catalytic pyrolysis; Activated carbon; Optimization; Oil production.*

Graphical abstract

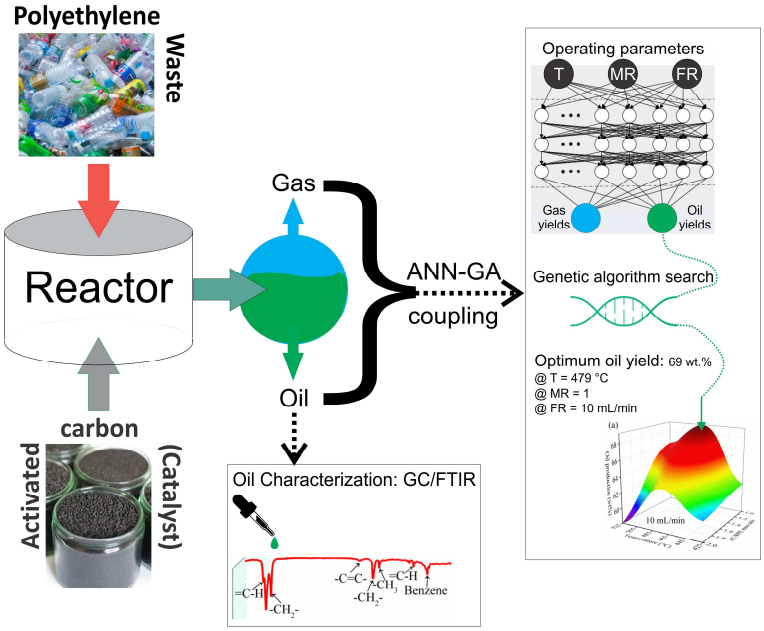

1. Introduction

Municipal solid waste (MSW) increases by ~2.01 billion tons per year due to global urbanization and population growth [1]. It has been reported that ~33 % of MSW is not

adequately managed [2]. Waste plastics account for a large proportion (5.6–27.6 wt%) of MSW [3]. Moreover, waste polyethylene (WPE) takes up the most significant proportion (38–62 wt%) of plastic in MSW [4]. Mass production of plastics and improper handling of waste plastics has led to a waste plastic crisis [5]. For example, landfilling would generate microplastics that harm ecosystems and living things [6]. In terms of the incineration of waste plastics, it causes a large amount of greenhouse gas emissions [7]. Therefore, it is necessary to adopt appropriate methods to dispose of waste plastics, WPE in particular.

Pyrolysis, without the presence of oxygen, is a promising method to convert WPE into value-added oil, gas, and char [8][9]. The pyrolysis oil is considered a substitute for commercial gasoline or diesel, so it has aroused the research interest of many researchers [5][10][11]. In the absence of catalysis, the WPE pyrolysis oil contains a large proportion of macromolecular wax that is solid at room temperature [12][13][14]. To be a suitable alternative to commercial fuels, researchers use catalysts to improve the quality of WPE pyrolysis oil.

It has been reported that activated carbon (AC) could effectively reduce wax in WPE pyrolysis oil. Duan et al. [15] reported that low-density PE could be pyrolyzed with AC (mass ratio of 1:1) at 550 °C to obtain ~45 wt% pyrolysis oil containing only C8–C16 hydrocarbons. Huo et al. [16] used AC to catalytically pyrolyze low-density PE (mass ratio of 2:1) at 500 °C to obtain 56.0 wt% oil, which was 100 % jet fuel. Zhang et al. [11] also recovered 54.0 wt% high-quality oil from low-density PE ex-situ catalytic pyrolysis with AC under the AC/low-density PE mass ratio of 2 and 571 °C. Besides, Zhang et al. [17] also found that AC

could enhance the aromatics' selectivity in the oil obtained from co-pyrolysis of biomass and high-density PE.

It can be concluded that the WPE pyrolysis oil could be upgraded by catalytic pyrolysis in the presence of AC. The effects of temperature and AC/WPE mass ratio on the yield and composition of WPE pyrolysis oil have also been comprehensively investigated. Nevertheless, according to [14][18], the flow rate of carrier gas is also a significant parameter, determining the oil yield and composition to a great extent. However, few studies were conducted to investigate the interactions of temperature and carrier gas flow rate on the WPE-AC catalytic pyrolysis oil yield to the best of our knowledge. Therefore, this study investigates the effect of AC/WPE mass ratio on the WPE catalytic pyrolysis affected by two operating parameters: the temperature and flow rate of carrier gas. Based on the mentioned studies, the target ranges for the temperature, the flow rate of carrier gas, and the AC/WPE mass ratio are 425–525 °C, 10–30 mL/min, and 1–2, respectively.

Since the correlation of the operating parameters and AC/WPE mass ratio is expected to be ill-posed, the methodology (proposed by Pan et al. [14]) of artificial neural network (ANN) coupled with a genetic algorithm (GA) is used to establish the mathematical expression to estimate oil yield under different conditions and then maximize the oil yield. The recovered oils are characterized by Fourier-transform infrared spectroscopy (FTIR) and gas chromatography/mass spectrometry (GC/MS). The main functional groups and components of the oil are analyzed under different operating parameters and AC/WPE mass ratios.

2. Experiments and methods

2.1. Materials

WPE (~3 mm particles) was recovered from MSW and provided by Zhoushan Jinke Renewable Resources Co., China. The AC sample was purchased from Sigma-Aldrich, Germany (100 mesh, CAS: 7440-44-0). The AC's BET surface area, average pore diameter, and average particle size are 876.45 m^2/g, 3.33 nm, and 19.27 μm, respectively [19].

Fig. 1 shows the thermogravimetric analysis of WPE. The sample was heated from 20 °C to 550 °C at a heating rate of 6 °C/min. 2.81 wt% of residue remained after the thermogravimetric analysis. The WPE's onset, end, and maximum degradation temperatures [20] were 452.1 °C, 494.1 °C, and 474.9 °C, respectively. Moreover, the maximum mass loss rate was 21.44 wt%/min.

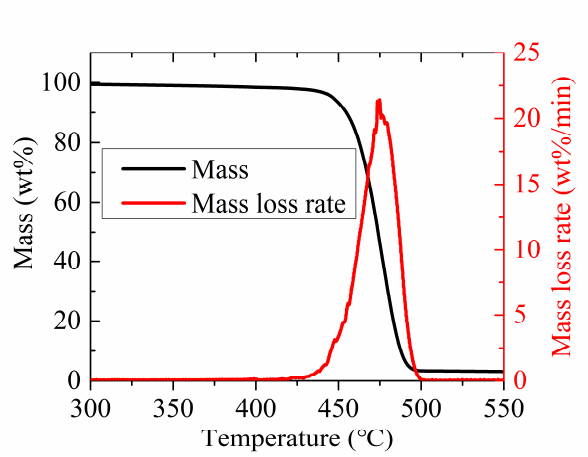

Fig. 1. Thermogravimetric analysis of WPE.

2.2. Experiments

Fig. 2 shows the experimental setup for ex-situ catalytic pyrolysis of WPE with AC. Nitrogen is severed as the purge gas (purge for 30 min under 100 mL/min) to create the

oxygen-free atmosphere for WPE-AC catalytic pyrolysis. The flow rate of nitrogen is controlled by the gas flow controller with the range of 0–250 mL/min. The pyrolysis is carried out in a 99% Al_2O_3 crucible (Φ40 mm × 60 mm, wall thickness 3 mm) placed in a 200 mL reactor. As shown in Fig. 1, ~2 g of WPE is evenly spread on the crucible bottom. The 2nd, 3rd, and fourth layers are quartz wool, AC, and quartz wool. The reactor is heated to the target temperature under 6 °C/min and stays at the target temperature for 20 min. The pyrolysis oil is cooled by the water-chiller condenser and condensed in the glass bottles placed in a mixture of ice and water. A 10 L gas bag is used to collect the pyrolysis gas.

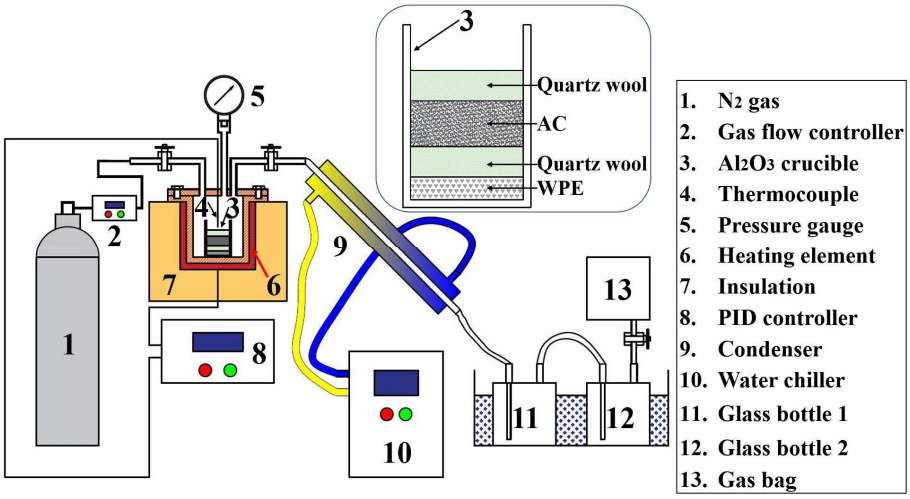

Fig. 2. Experimental setup for ex-situ catalytic pyrolysis of WPE with AC.

Table 1 shows the experimental design of ex-situ catalytic pyrolysis of WPE with AC based on the central-composite design [11][14]. The temperature, AC/WPE mass ratio, and flow rate of carrier gas were investigated in the ranges of 425–525 °C, 1–2, and 10–30 mL/min, respectively. Experiments of R1–R16 were carried out to obtain the training data for ANN-GA, and V1–V6 were conducted to gain the testing data.

Table 1

Experimental design of ex-situ catalytic pyrolysis of WPE with AC.

Run	Temperature (°C)	AC/WPE mass ratio	Carrier gas flow rate (mL/min)
R1	425	1	10
R2	425	1	30
R3	425	1.5	20
R4	425	2	10
R5	425	2	30
R6	475	1	20
R7	475	1.5	10
R8	475	1.5	20
R9	475	1.5	30
R10	475	2	20
R11	475	2	30
R12	525	1	10
R13	525	1	30
R14	525	1.5	20
R15	525	2	10
R16	525	2	30
V1	450	1	10
V2	450	1.25	25
V3	450	1.75	15
V4[a]	479	1	10
V5	500	1.25	25
V6	500	1.75	15

[a] Conditions optimized by ANN-GA.

2.3. Characterization methods for recovered oil

FTIR (Thermo Nicolet 6700) and GC/MS (Thermo Scientific TRACE 1300/1310 coupled Thermo Fisher TSQ 9000) analyses were conducted to identify the recovered oils' functional groups and specific compositions. The operating details are wholly described in the previous study [14].

2.4. ANN-GA

Fig. 3 shows the flow schematic of ANN coupled with GA, which has been described in detail in previous studies [14][21][22]. This study adopted ANN-GA to investigate the triplet of parameters: pyrolysis temperatures, AC/WPE mass ratios, and flow rates of carrier gas. ANN trained the experimental gas and oil yields under the triplet combination, and then the mathematical expressions of gas and oil yields were expressed in terms of the triplet of parameters. Subsequently, the oil yield was optimized by GA to obtain the highest value.

In order to verify the applicability of ANN-GA, this study used ANN-GA to optimize the required heat and exergy efficiency during the WPE gasification process [23]. Hasanzadeh et al. [23] investigated the interactions of temperature and steam to polyethylene waste ratio (S/P ratio) on the WPE gasification's required heat and exergy efficiency. They used the response surface methodology (RSM) to establish the mathematical expressions of required heat and exergy efficiency expressed in terms of temperature and S/P ratio. A total of 13 sets of tests were conducted to obtain the training data. The comparison of the predicted results of RSM and ANN-GA was described in detail in Appendix A. The ANN-GA predicted results were more consistent with the original data and more accurate than the RSM predicted ones. It can be concluded that ANN-GA can predict and optimize other researches' data.

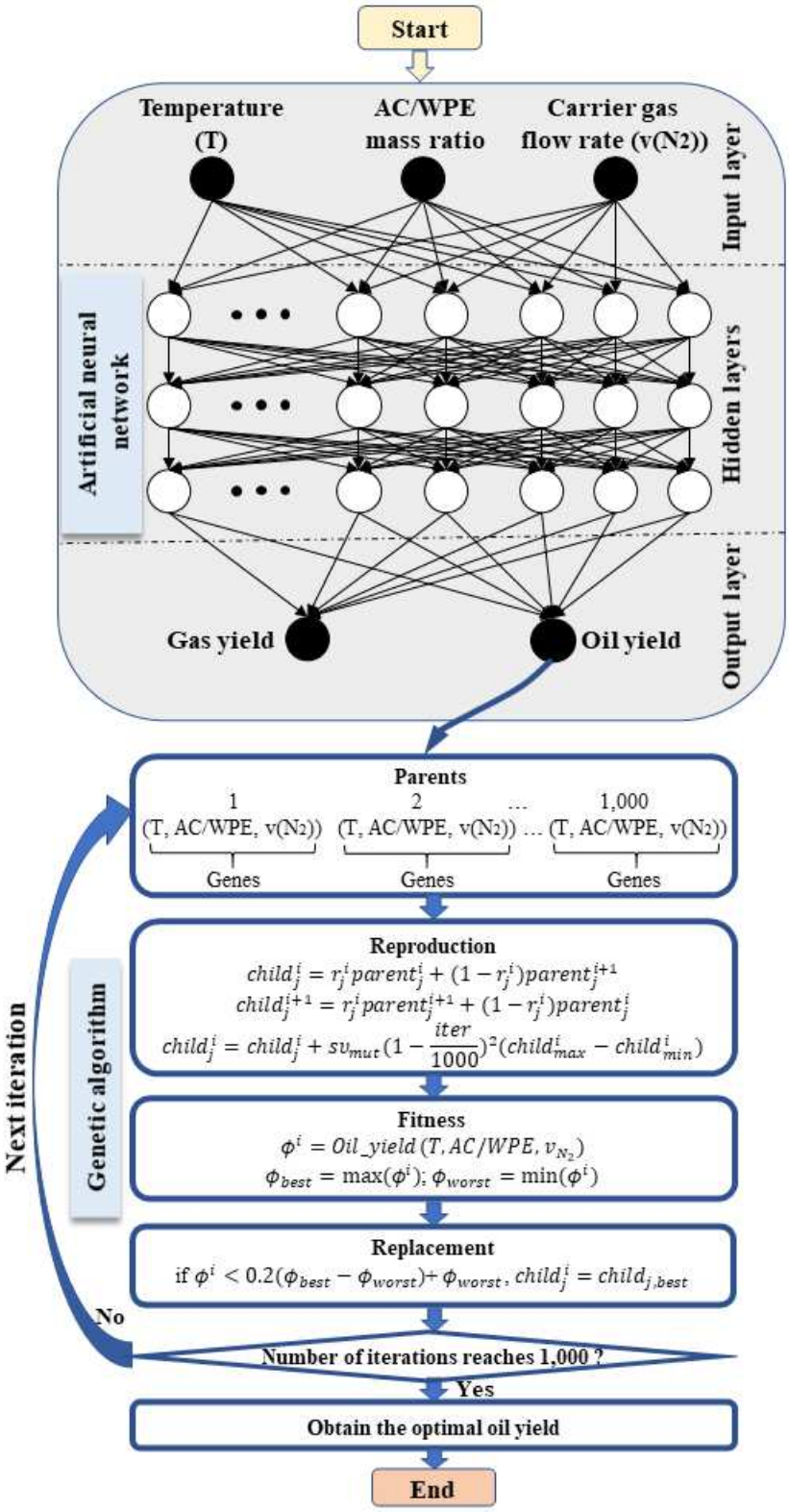

Fig. 3. Flow schematic of ANN coupled with GA for the context of the present work.

3. Results and discussion

3.1. Accuracy of ANN

Fig. 4 shows the experimental and the ANN predicted oil and gas productions from the WPE-AC catalytic pyrolysis in the training and testing sets. The experimental oil and gas yields oscillated between 56.31–69.63 wt% and 21.18–42.46 wt%, respectively. It is noteworthy that the WPE thermal pyrolysis oil yield (65.31–83.50 wt%) was higher than the WPE-AC catalytic pyrolysis one, whereas the WPE thermal pyrolysis gas yield (11.50–18.59 wt%) was lower than the WPE-AC catalytic pyrolysis one within the same temperature range of 425–525 °C [14]. It was because that the WPE could be decomposed into the shorter-chain hydrocarbons in the presence of catalysts [24]. Santos et al. [25] recovered approximately 21–59 wt% oil and 16–50 wt% gas from the high-density PE catalytic pyrolysis with H-ZSM-5 (1 wt%) in a relatively lower temperature range 430–470 °C. Zhang et al. [11] recovered 38.5–73.0 wt% high-quality oil and 10.9–44.8 wt% gas from the low-density PE catalytic pyrolysis with AC in the temperature range of 430–571 °C. These results were close to the values presented in this study.

Fig. 4 also illustrates the absolute relative errors (AREs) between the experimental and the ANN predicted oil and gas yields. It could be seen that the predicted oil yields (AREs within 3.1 %) were more accurate than the predicted gas yields (AREs within 11.8 %). It might be because the gas production was calculated by the difference method, which caused the accumulation of errors in gas yield [14]. Moreover, the R^2 values and average AREs between the experimental and ANN predicted values were 0.9992 and 0.60 %, 0.9830 and 5.01 % in the training and testing tests. The high R^2 values and low average AREs revealed the high

accuracies of ANN-predicted oil and gas yields.

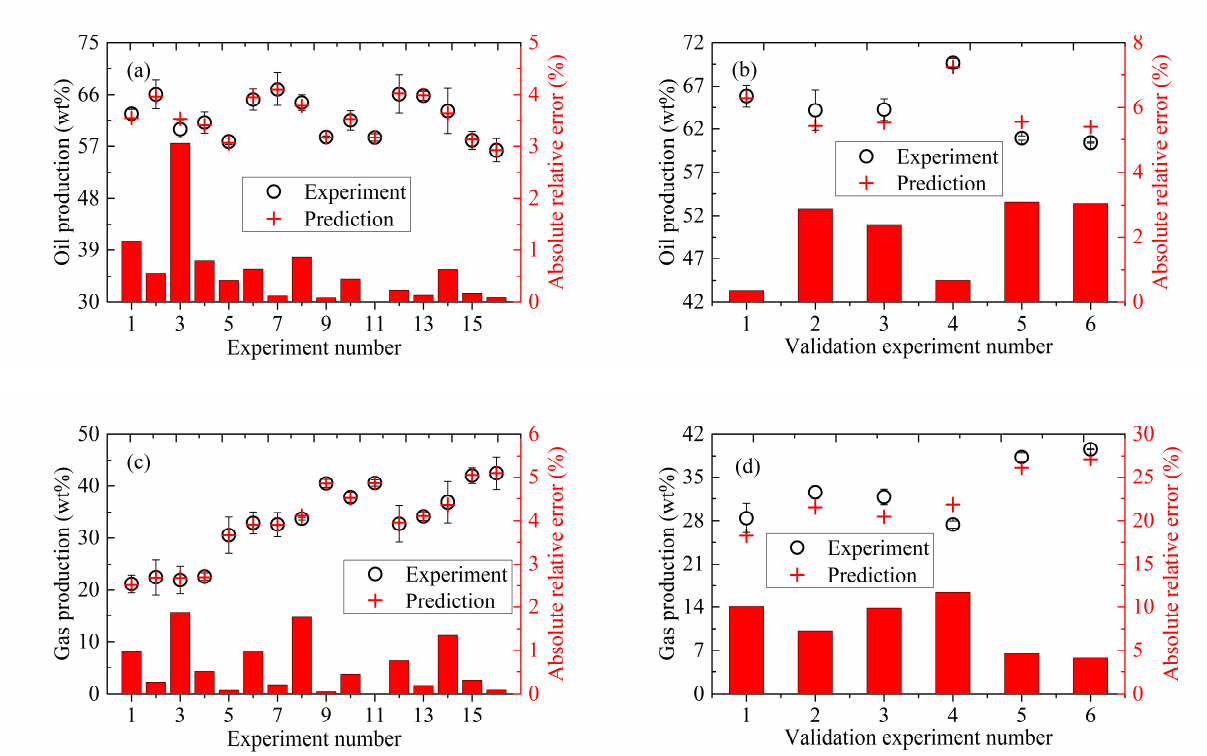

Fig. 4. Experimental and ANN predicted oil and gas productions in training and testing sets: (a) Oil production in the training set; (b) Oil production in the testing set; (c) Gas production in the training set; (d) Gas production in the testing set.

3.2. Interactions of temperature and AC/WPE mass ratio

Fig. 5 shows the interactions of temperature and AC/WPE mass ratio on oil and gas productions under different carrier gas flow rates. The variation ranges of oil and gas productions under different carrier gas flow rates are tabulated in Table 2. It can be found that under the highest AC/WPE mass ratio of 2, the oil production increased with the increasing temperature in the range of 425–475 °C, regardless of the variation of carrier gas flow rate. Higher temperatures aggravated the random scissions of WPE, resulting in more volatile

products [26]. Therefore, gas production was also enhanced when the temperature increased [27]. However, enhancing temperature above 475 °C intensified the secondary cracking of pyrolysis oil, leading to a decrease in oil production and an increase in gas production [28]. It is noteworthy that the effect of temperature on oil and gas yields was more complicated under 30 mL/min (Figs. 5e–f). Under the lowest AC/WPE mass ratio of 1, the oil production decreased from 65.68 wt% at 425 °C, reached the minimum yield of 58.53 wt% at 475 °C, and increased thenceforth. The gas recondensation might cause an increase in oil yield at higher temperatures [29]. In this perspective, the gas yield decreased by 6.15 wt% (from 40.40 wt% to 34.25 wt%) as the temperature increased from 475 °C to 525 °C, which might be ascribed to promoting the Diels-Alder reaction for gas aromatized by AC [30].

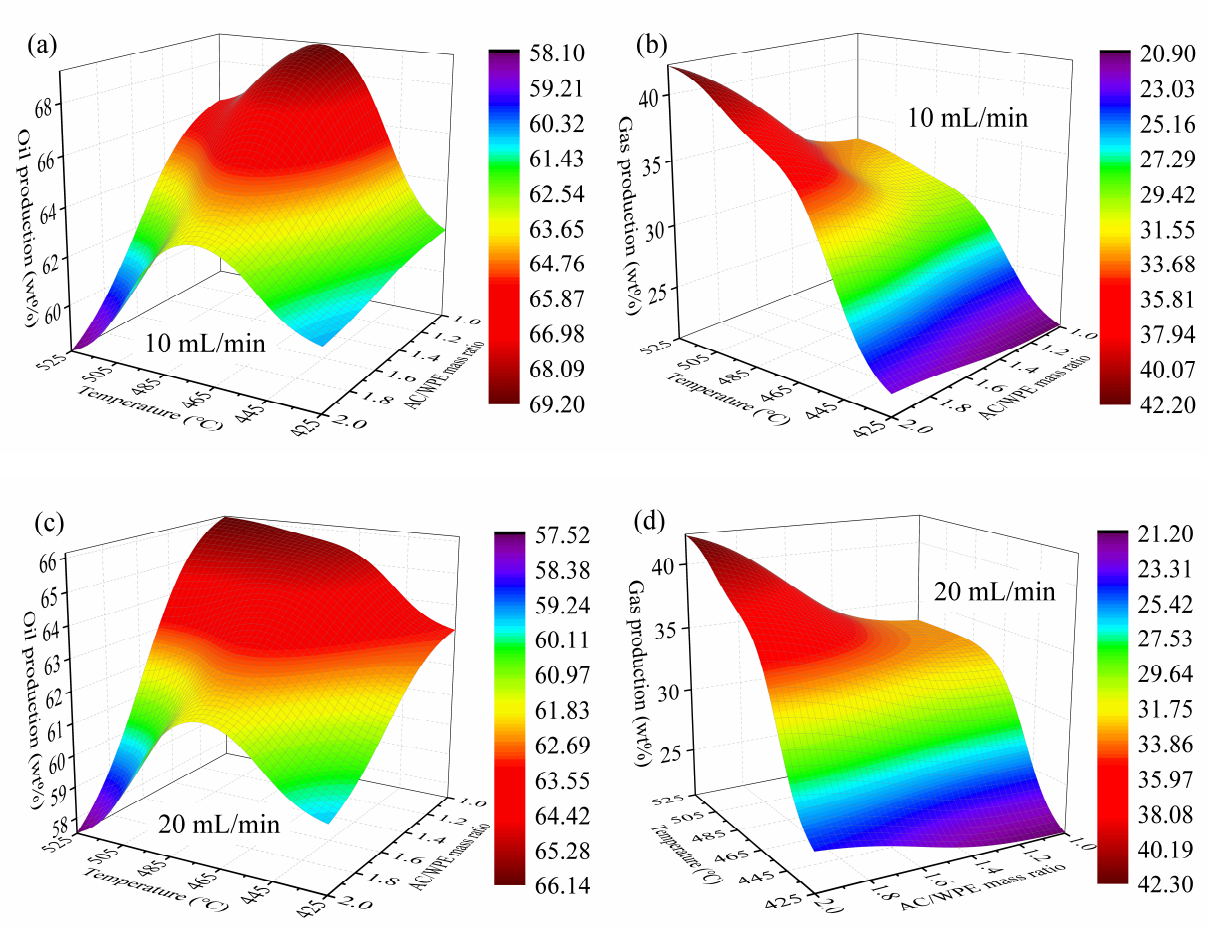

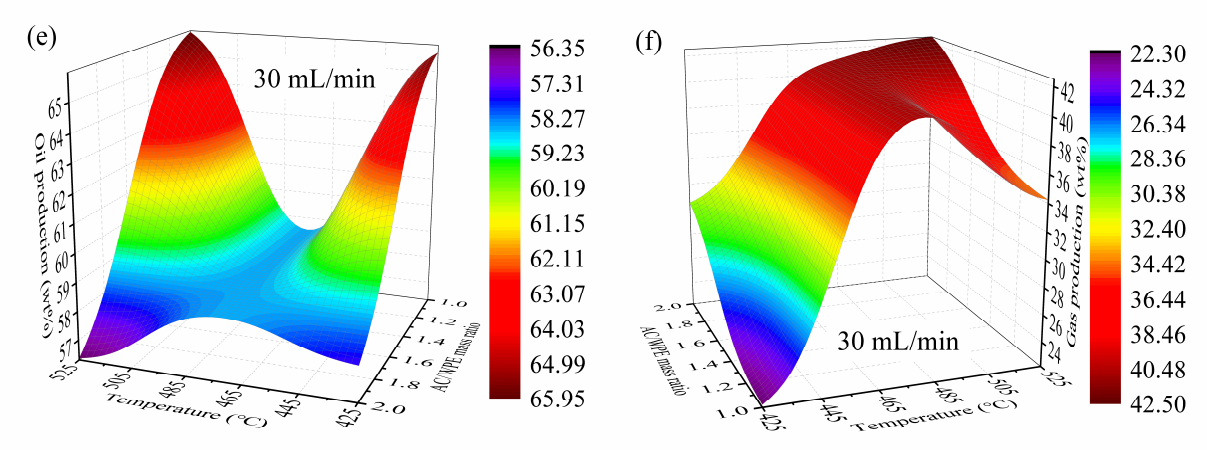

Fig. 5. Interactions of temperature and AC/WPE mass ratio on oil and gas productions under different carrier gas flow rates: (a) Oil production under 10 mL/min; (b) Gas production under 10 mL/min; (c) Oil production under 20 mL/min; (d) Gas production under 20 mL/min; (e) Oil production under 30 mL/min; (f) Gas production under 30 mL/min.

Table 2

WPE catalytic pyrolysis oil and gas productions under different carrier gas flow rates.

Temperature: 425–525 °C; AC/WPE mass ratio: 1.0–2.0			
Yield	Under 10 mL/min	Under 20 mL/min	Under 30 mL/min
Oil	58.12–69.16 wt%	57.53–66.13 wt%	56.36–65.90 wt%
Gas	20.97–42.11 wt%	21.29–42.20 wt%	22.39–42.50 wt%

3.3. Interactions of AC/WPE mass ratio and carrier gas flow rate

Fig. 6 illustrates the interactions of AC/WPE mass ratio and carrier gas flow rate on oil and gas productions under different temperatures. Table 3 exhibits the variation ranges of oil and gas productions under different temperatures. It can be concluded that a higher AC/WPE mass ratio would reduce oil production and enhance gas production, regardless of the variations of carrier gas flow rate and temperature. More catalytic sites exacerbated WPE

backbone cracking and oil secondary cracking, thereby led to a decrease in oil yield and an increase in gas yield [11][31]. The AC/WPE mass ratio faintly impacted the oil production under 10mL/min and 425 °C (Fig. 6a). The oil yield merely decreased by 1.27 wt% as the AC/WPE mass ratio increased. It may be ascribed to that partial polyene radicals also formed light oils via rearrangement, cyclization, and aromatization in the catalytic sites [29][32]. However, as carrier gas flow rate increased to 30 mL/min (Fig. 6b), oil secondary cracking was more intense than gas recondensation reaction [14], resulted in a dramatic reduction (of 8.11 wt%) of oil yield as the AC/WPE mass ratio increased.

The AC/WPE mass ratio had an inconspicuous impact on oil and gas yields under 30 mL/min and 475 °C (Figs. 5c–d). Fan et al. [10] also found that the oil yield almost unchanged when the MgO/LDPE mass ratio enhanced from 1/10 to 1/3. They attributed it to the fact that excess catalyst would not further promote the secondary cracking reaction. On the other hand, higher carrier gas flow rates would lead to heavier oil production [14]. It might block the AC's pores to decrease the catalyst activity, which led to the practically constant oil and gas yields as the AC/WPE mass ratio increased [11]. However, increasing the AC/WPE mass ratio led to a decrease of 5.70 wt% in oil yield and an increase of 6.47 wt% in gas yield under 10 mL/min and 475 °C. Moreover, the oil yield decreased by approximately 8 wt%, and the gas yield enhanced by approximately 8wt% when the AC/WPE mass ratio increased from 1 to 2 under 525 °C, regardless of carrier gas flow rate's variation. It indicated that higher AC/WPE mass ratios could promote the oil secondary cracking for the oil consumption and the gas formation by providing more active sites [33].

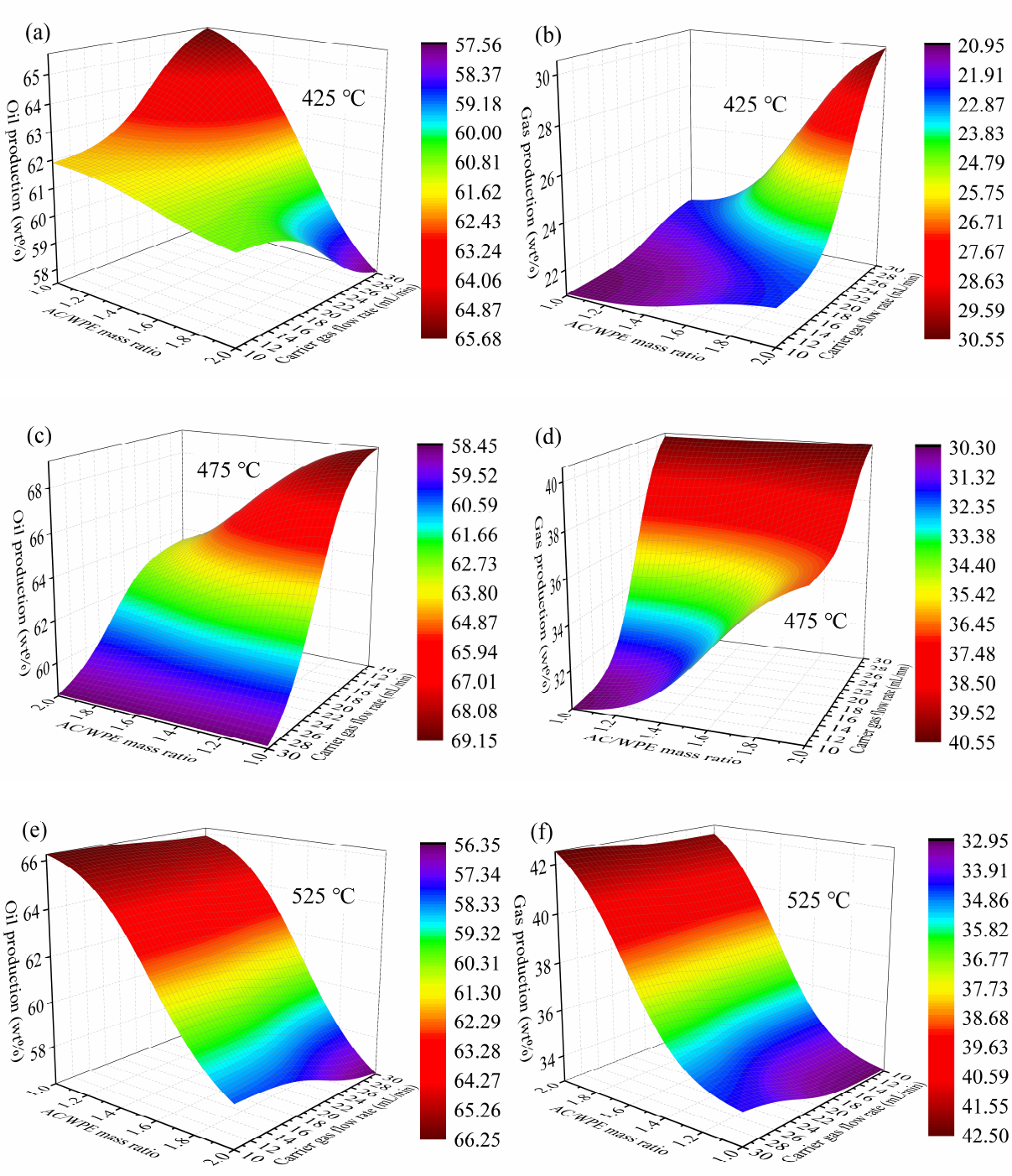

Fig. 6. Interactions of AC/WPE mass ratio and carrier gas flow rate on oil and gas productions under different temperatures: (a) Oil production under 425 °C; (b) Gas production under 425 °C; (c) Oil production under 475 °C; (d) Gas production under 475 °C; (e) Oil production under 525 °C; (f) Gas production under 525 °C.

Table 3

WPE catalytic pyrolysis oil and gas productions under different temperatures.

Carrier gas flow rate: 10–30 mL/min; AC/WPE mass ratio: 1.0–2.0			
Yield	Under 425 °C	Under 475 °C	Under 525 °C
Oil	57.57–65.68 wt%	58.48–69.10 wt%	56.36–66.24 wt%
Gas	20.97–30.52 wt%	30.31–40.54 wt%	32.99–42.50 wt%

3.4. Interactions of carrier gas flow rate and temperature

Fig. 7 shows the interactions of carrier gas flow rate and temperature on oil and gas productions under different AC/WPE mass ratios. Table 4 tabulates the variation ranges of oil and gas productions under different AC/WPE mass ratios. As shown in Figs. 7a (AC/WPE mass ratio = 1), 6c (AC/WPE mass ratio = 1.5), and 6e (AC/WPE mass ratio = 2), enhancing the flow rate of carrier gas led to an increase of 3.78 wt%, an increase of 0.11 wt%, and a reduction of 3.06 wt% in oil yields under the lowest temperature of 425 °C, respectively. More significant carrier gas flow rates could inhibit the oil secondary cracking, thereby increased the oil yield [18]. On the other hand, increasing the flow rate of carrier gas would purge the produced volatiles out of the reactor faster, thereby suppressing the formation of light oils from the partial polyene radicals via rearrangement, cyclization, and aromatization [11][32]. As the flow rate of carrier gas increased, the oil yield would enhance when the gas recondensation reaction was more violent than the oil secondary cracking, while it would reduce as the oil secondary cracking dominated. It can be seen that the secondary cracking of oil was dominant in the middle-temperature range of 450–500 °C. Therefore, enhancing the flow rate of carrier gas led to a decrease in oil yield and an increase in gas yield under all

AC/WPE mass ratios. However, the flow rate of carrier gas became an inconspicuous parameter on both oil and gas yields when the temperature was higher than 500 °C. It might be ascribed that higher temperature would increase the heavy fraction in oil [14] and decrease the alkenes in gas [34]. Both the secondary cracking of oil and the recondensation of gas were at low reactivity, and thereby the oil and gas yields did not change with the flow rate of carrier gas under higher temperatures.

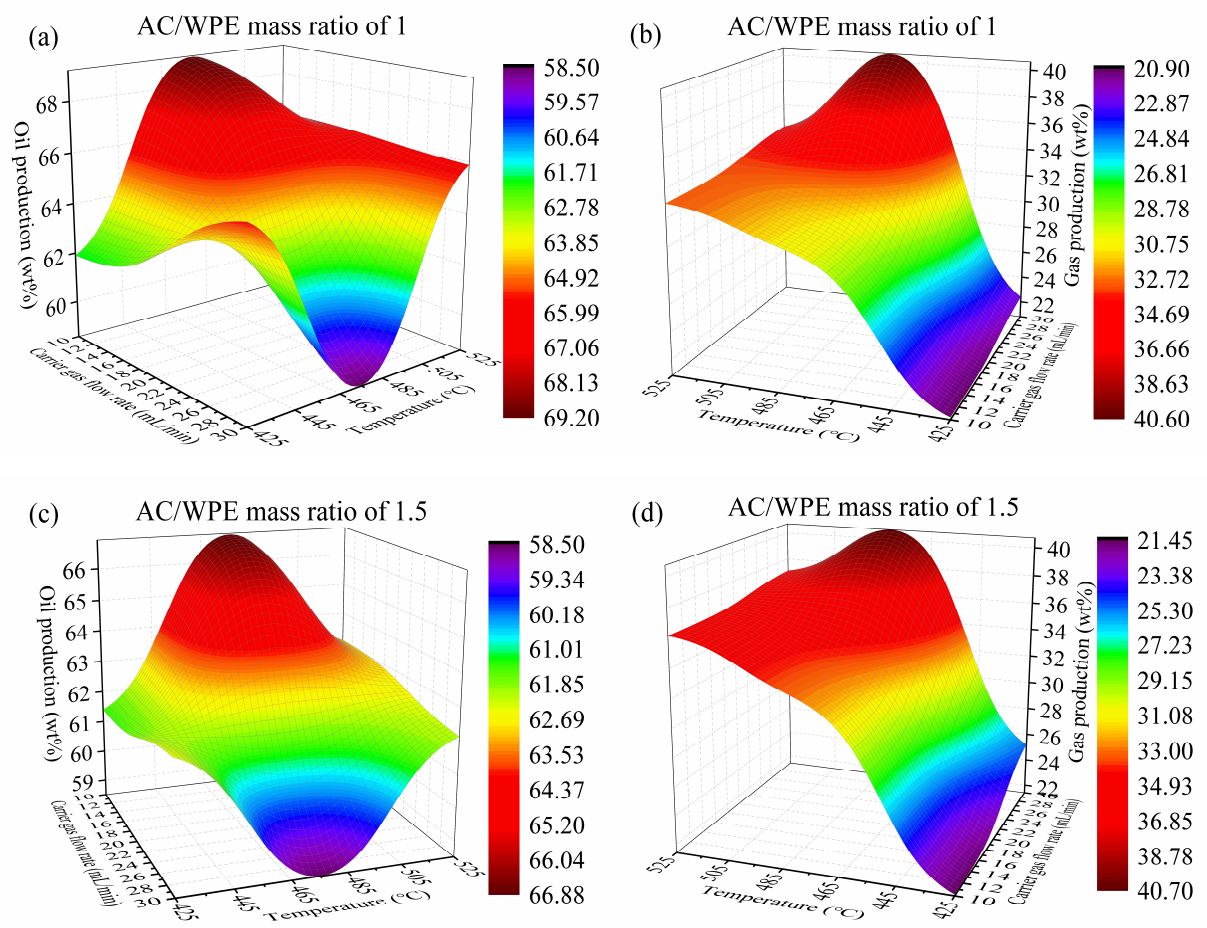

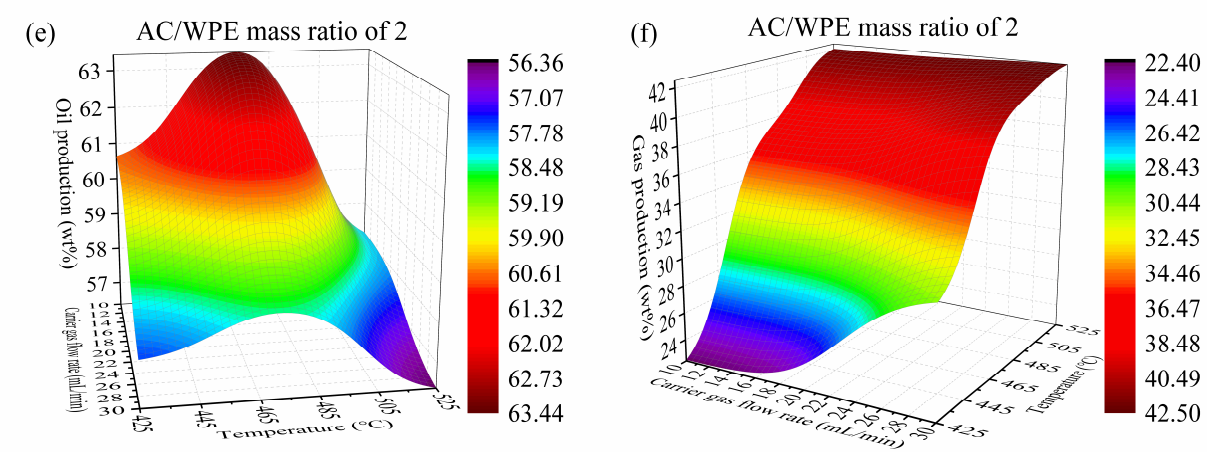

Fig. 7. Interactions of carrier gas flow rate and temperature on oil and gas productions under different AC/WPE mass ratios: (a) Oil production under AC/WPE mass ratio of 1; (b) Gas production under AC/WPE mass ratio of 1; (c) Oil production under AC/WPE mass ratio of 1.5; (d) Gas production under AC/WPE mass ratio of 1.5; (e) Oil production under AC/WPE mass ratio of 2; (f) Gas production under AC/WPE mass ratio of 2.

Table 4

WPE catalytic pyrolysis oil and gas productions under different AC/WPE mass ratios.

Temperature: 425–525 °C; Carrier gas flow rate: 10–30 mL/min			
Yield	Under AC/WPE mass ratio of 1	Under AC/WPE mass ratio of 1.5	Under AC/WPE mass ratio of 2
Oil	58.53–69.16 wt%	58.51–66.86 wt%	56.36–63.42 wt%
Gas	20.97–40.58 wt%	21.49–40.69 wt%	22.48–42.50 wt%

3.5. ANN-GA optimization

Fig. 8 shows the ANN-GA optimization process and optimal conditions for oil production through the ex-situ catalytic pyrolysis of WPE with AC. As shown in Fig. 8a, the highest oil production was determined at the 200th iteration. Fig. 8b illustrates that the optimal oil

production calculated by ANN-GA was 69.16 wt% under 479 °C, the AC/WPE mass ratio of 1, and 10 mL/min. It indicated that the moderate temperature (≤ 500 °C) [30][35], the low AC/WPE mass ratio [36][37], and the low flow rate of carrier gas [38][39] were beneficial to oil production. The experimental oil yield was 69.63 wt% under the optimal parameters. The absolute relative error was 0.67 % between the experimental and the ANN-GA determined oil yields, which exhibited the high accuracy of ANN-GA. Moreover, the optimal temperature for WPE thermal pyrolysis was 488 °C [14], a value higher than the optimal temperature for WPE-AC catalytic pyrolysis. Therefore, it can be concluded that the presence of AC could decrease the optimal pyrolysis temperature of WPE.

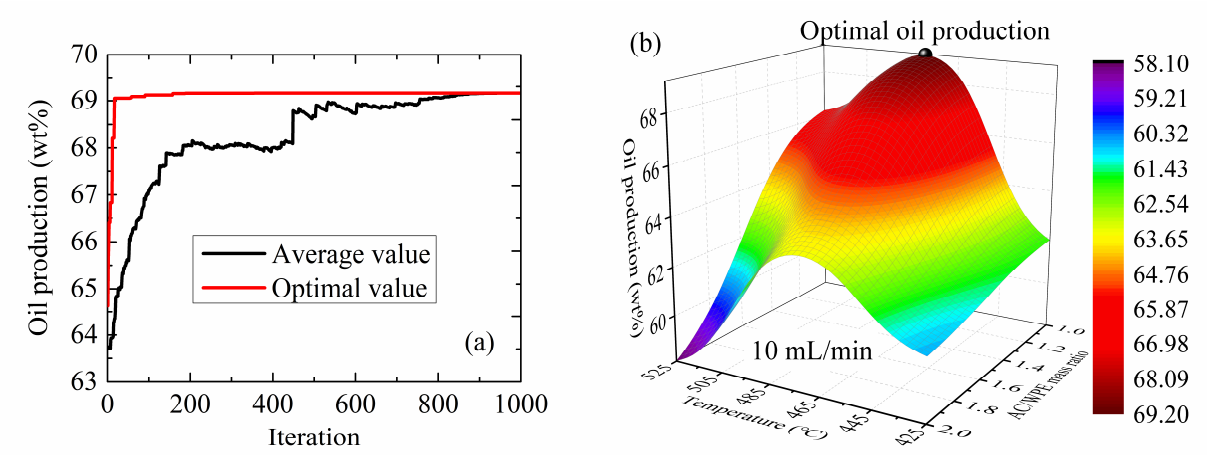

Fig. 8. Optimal conditions optimized by ANN-GA for maximum oil production: (a) Optimization process; (b) Optimal conditions for oil production.

3.6. FTIR analysis

Fig. 9 shows the FTIR spectrum of oil samples under different conditions (oil samples of R3, R6, R7, R8, R9, R10, and R14). It can be seen that the oil's FTIR characteristic peaks did not change with the temperature, the AC/WPE mass ratio, and the flow rate of carrier gas. The

oils were composed of alkenes, naphthenes, alkanes, and aromatic hydrocarbons, which indicated that WPE-AC catalytic pyrolysis underwent random and Beta scissions [25], hydrogen transfers (both inter- and intra-molecular) [40], and molecular cyclization and aromatization [41].

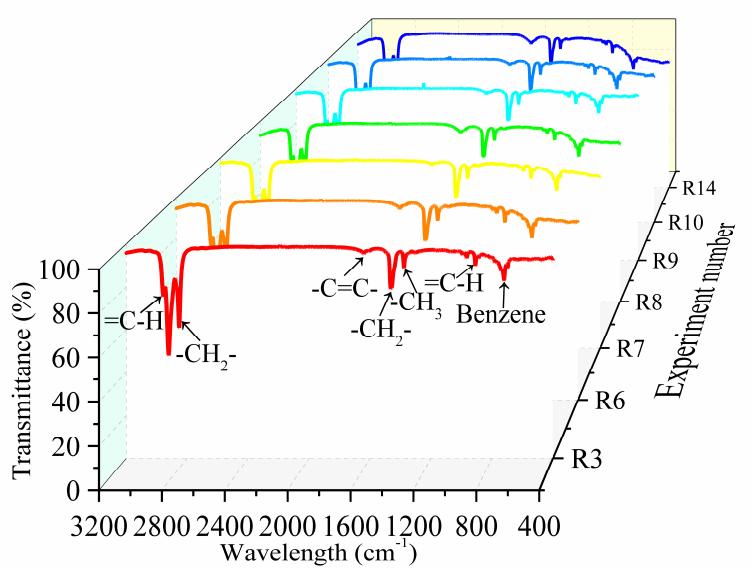

Fig. 9. FTIR spectrum of oil samples under different conditions.

3.7. GC-MS analysis

Fig. 10 shows carbon number distribution and fractions of the WPE-AC catalytic and thermal pyrolysis oils. The thermal and catalytic pyrolysis (R14) were performed under the same operating parameters (525 °C, 20 mL/min, 20 min). It can be seen that the WPE thermal pyrolysis oil was composed of C7–C36 hydrocarbons with a large proportion of C21–C24 and C30 (> 6 %) [14], while the WPE-AC catalytic pyrolysis oil was composed of C8–C33 hydrocarbons with a large proportion of C9–C12 and C15 (> 7 %). AC could accelerate the hydrogen-ion abstraction reaction of the WPE hydrocarbon long chain to form more

carbonium-ion free radicals, which was conducive to generating shorter chain hydrocarbons with lower carbon numbers [42][43]. Therefore, as shown in Fig. 10b, the light (C7–C11) and middle (C12–C20) frictions significantly increased from 4.55 % to 27.40 %, from 31.27 % to 57.24 %, and the heavy friction (> C20) reduced dramatically from 64.18 % to 15.36 % in the presence of AC.

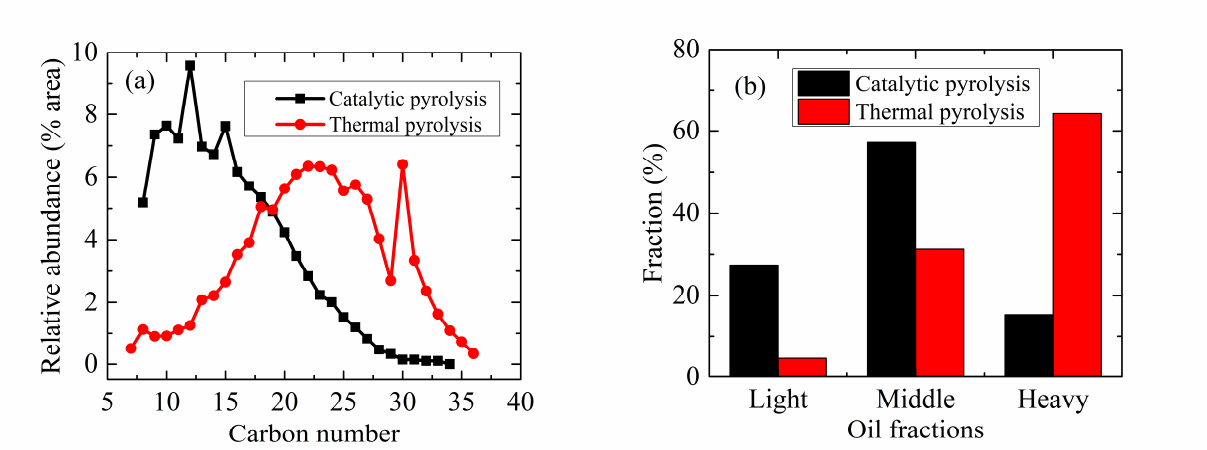

Fig. 10. Carbon number distribution and fractions of the WPE catalytic and thermal pyrolysis oils: (a) Carbon number distribution; (b) Oil fractions.

3.7.1. Effect of temperature on carbon number distribution and oil fractions

Fig. 11 shows the effect of temperature on the carbon number distribution and the fractions of WPE-AC catalytic pyrolysis oil. As depicted in Fig. 11a, the carbon number distribution trends were similar under different temperatures. Hydrocarbons with the carbon numbers of C8–C18 were all greater than 4 %, which together accounted for ~75 % of the WPE-AC catalytic pyrolysis oils. Moreover, the hydrocarbons with carbon numbers above C30 only took up ~1 % in oils under all operating temperatures.

As shown in Fig. 11b, the light-fraction increased from 28.70 % to 35.96 % as the

temperature enhanced from 425 °C to 475 °C, whereas it decreased to 27.40 % as the temperature continuously increased to 525 °C. The middle-fraction firstly decreased from 55.09 % to 46.70 % when the temperature increased from 425 °C to 475 °C, while it increased to 57.24 % under 525 °C. The heavy-fraction oscillated in a narrow range of 15.36–17.34 %, which was not significantly affected by the temperature [44]. Therefore, it could conclude that improving the temperature from 425 °C was beneficial to convert the WPE-AC catalytic pyrolysis oil's middle-fraction to light-fraction at first, thereby leading to an increase in the light-fraction and a decrease in the middle-fraction [35][41][45]. However, continuously increasing the temperature to 525 °C resulted in the over-cracking of light-fraction, which contributed to the reduction of light-fraction and the enhancement of middle-fraction in the WPE-AC catalytic pyrolysis oil [35][46].

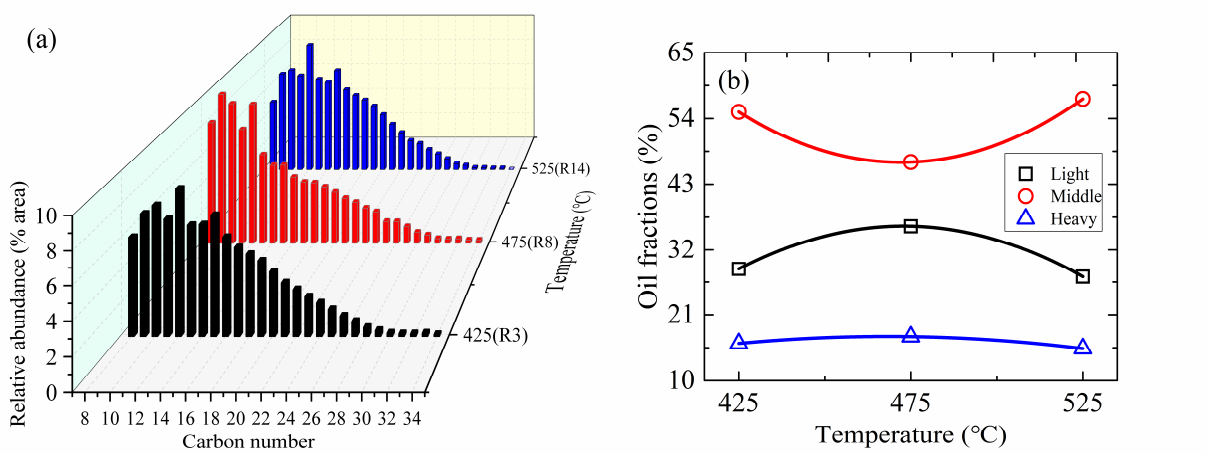

Fig. 11. Effect of temperature on the carbon number distribution and the fractions of WPE catalytic pyrolysis oil: (a) Carbon number distribution; (b) Oil fractions.

3.7.2. Effect of AC/WPE mass ratio on carbon number distribution and oil fractions

Fig. 12 demonstrates the effect of AC/WPE mass ratio on the carbon number distribution

and the fractions of WPE-AC catalytic pyrolysis oil. As illustrated in Fig. 12a, the oil under the AC/WPE mass ratio of 1.5 had more hydrocarbons with the carbon numbers of C8–C11 than the oils under the AC/WPE mass ratios of 1 and 2. The oil under the AC/WPE mass ratio of 2 had the most abundant hydrocarbons with the carbon numbers of C12–C15. On the other hand, the highest content of hydrocarbons above C15 was obtained under the lowest AC/WPE mass ratio of 1.

Consequently, as depicted in Fig. 12b, the light-fraction enhanced from 23.46 % to 35.96 % as the AC/WPE mass ratio increased from 1 to 1.5, while decreased to 29.18 % as the AC/WPE mass ratio sequentially enhanced to 2. The middle-fraction initially reduced from 55.48 % to 46.70 % when the AC/WPE mass ratio improved from 1 to 1.5, whereas it increased to 53.56 % under the AC/WPE mass ratio of 2. Moreover, the heavy-fraction gradually decreased from 21.06 % to 17.26 % as the AC/WPE mass ratio enhanced. The reductions of middle-fraction and heavy-fraction and the enhancement of light-fraction might be attributed to the sufficient acid sites for the secondary cracking of middle-fraction and heavy-fraction in oil when the AC/WPE mass ratio enhanced from 1 to 1.5 [15]. However, the excessive acid sites might conduce to the over-cracking of oil's light-fraction, which correspondingly led to an increase in gas production [15][45].

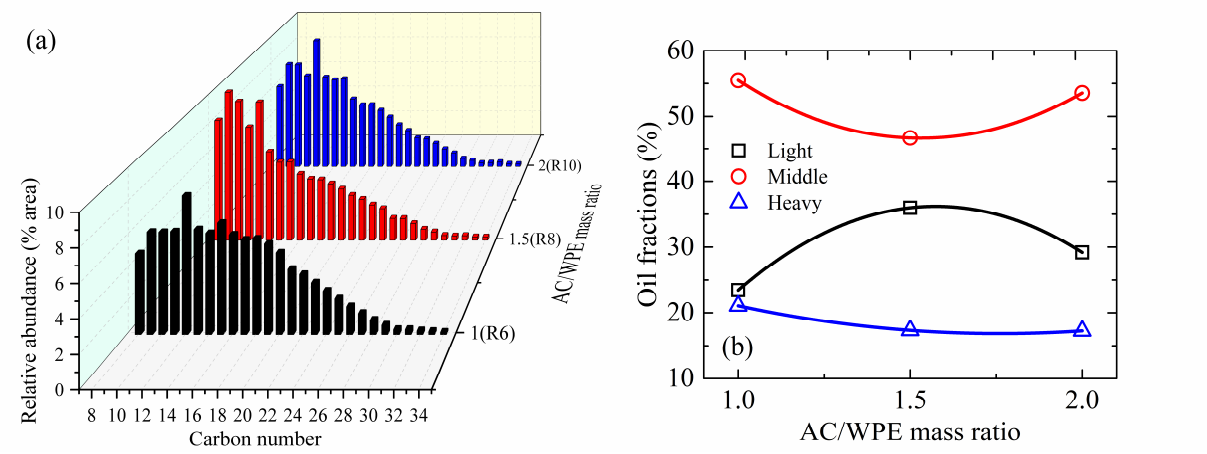

Fig. 12. Effect of AC/WPE mass ratio on the carbon number distribution and the fractions of WPE catalytic pyrolysis oil: (a) Carbon number distribution; (b) Oil fractions.

3.7.3. Effect of carrier gas flow rate on carbon number distribution and oil fractions

Fig. 13 illustrates the effect of carrier gas flow rate on the carbon number distribution and the fractions of WPE-AC catalytic pyrolysis oil. As shown in Fig. 13a, the hydrocarbons with carbon numbers of C8–C12 in the oil under 20 mL/min were richer than those in the oils under 10 mL/min and 30 mL/min. The oil under the lowest flow rate of carrier gas (10 mL/min) had the most abundant hydrocarbons with the carbon numbers of C14–C24 compared to the oils under 20 mL/min and 30 mL/min. In comparison, the highest content of hydrocarbons above C24 was obtained under the highest flow rate of carrier gas (30 mL/min), which together accounted for around 7 % in the WPE-AC catalytic pyrolysis oil.

Accordingly, as illustrated in Fig. 13b, the light-fraction increased from 19.46 % to 35.96 % as the flow rate of carrier gas enhanced from 10 mL/min to 20 mL/min, whereas reduced to 26.61 % as the flow rate of carrier gas subsequently enhanced to 30 mL/min. The middle-fraction firstly decreased from 59.40 % to 46.70 % as the flow rate of carrier gas

improved from 10 mL/min to 20 mL/min, while enhanced to 53.19 % under 30 mL/min. The heavy-fraction fluctuated between 17.34 % and 21.13 %, which was not significantly influenced by the flow rate of carrier gas. The enhancement of light-fraction and the reductions of middle-fraction and heavy-fraction might be ascribed to the suppression of the light-fraction's over-cracking as the flow rate of carrier gas enhanced from 10 mL/min to 20 mL/min [47]. However, the excessive flow rate of carrier gas shortened the residence time of volatile gas and suppressed the gas recondensation and the secondary cracking of middle-fraction and heavy-fraction, which further decreased the oil's light-fraction formation [47][48][49].

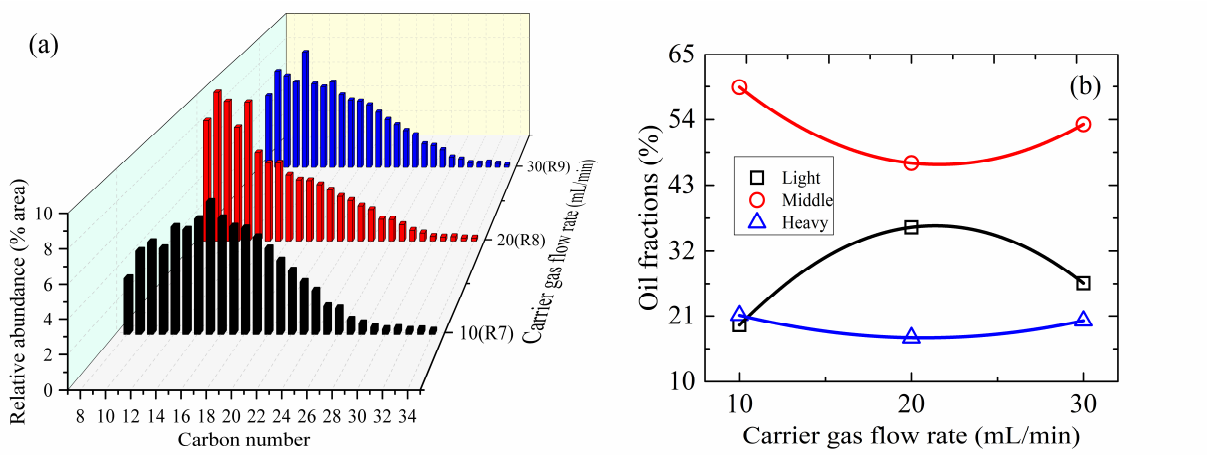

Fig. 13. Effect of carrier gas flow rate on the carbon number distribution and the fractions of WPE catalytic pyrolysis oil: (a) Carbon number distribution; (b) Oil fractions.

4. Conclusions

This study investigated the ex-situ catalytic pyrolysis of waste polyethylene (WPE) with activated carbon (AC). The pyrolysis experiments were carried out in a bench-scale semi-batch reactor. The operating parameters of temperature and carrier gas flow rate, and

AC/WPE mass ratio were investigated in the ranges of 425–525 °C, 1–2, and 10–30 mL/min, respectively. It was found that the operating parameters and AC/WPE mass ratio had complex interactions on the WPE-AC catalytic pyrolysis oil and gas yields. Therefore, a hybrid method of artificial neural network (ANN) coupled with genetic algorithm (GA) was used to establish the mathematical expressions of oil and gas yields under different conditions and optimize the conditions to obtain the highest oil yield. It should be noted that the correlations obtained in this study have application limitations delimited by the experimental apparatus and process conditions. Nonetheless, ANN-GA has been proved to have good robustness, which can provide guidance for industrial process optimization. The main findings and conclusions are outlined as follows.

- The oil production optimized by ANN-GA was 69.63 wt% under 479 °C, the AC/WPE mass ratio of 1, and 10 mL/min.
- The oils were composed of alkenes, naphthenes, alkanes, and aromatic hydrocarbons in the range of C8–C33.
- Improving the temperature from 425 °C was firstly beneficial to convert the middle-fraction into the light-fraction in the WPE-AC catalytic pyrolysis oil, while continuously increasing the temperature to 525 °C resulted in a decrease in the light-fraction and an increase in the middle-fraction.
- Increasing the AC/WPE mass ratio led to an increase in the light-fraction and a decrease in the middle-fraction when the AC/WPE mass ratio was low (1–1.5); However, the excessive AC/WPE mass ratio (1.5–2) decreased the light-fraction and increased the middle-fraction

in the pyrolysis oil.

- A lower carrier gas flow rate led to a higher proportion of light-fraction and lower middle- and heavy-fraction proportions.

Author Information

Corresponding Author *E-mail: gerald.debenest@toulouse-inp.fr

Competing Interest

The authors declare no competing financial interest.

Acknowledgments

This work was supported by the China Scholarship Council (CSC) program (No. 201906120036). Thanks are given to Dr. Yue ZAN from LCC-CNRS-UPS (Laboratoire de Chimie de Coordination du CNRS, Université Toulouse III - Paul Sabatier) for her assistance in the FTIR test and analysis.

References

[1] Z. Usmani, V. Kumar, S. Varjani, P. Gupta, R. Rani, A. Chandra. Municipal solid waste to clean energy system: a contribution towards sustainable development. S. Varjani, A. Pandey, E. Gnansounou, S.K. Khanal, S. Raveendran (Eds.), Resource Recovery from Wastes, Elsevier, Amsterdam, Netherlands (2020), pp. 217-231. https://doi.org/10.1016/B978-0-444-64321-6.00011-2.

[2] A.V. Shah, V.K. Srivastava, S.S. Mohanty, S. Varjani. Municipal solid waste as a sustainable resource for energy production: State-of-the-art review. J Environ Chem Eng, 9 (4) (2021), p. 105717. https://doi.org/10.1016/j.jece.2021.105717.

[3] Y.M. Wen, I.N. Zaini, S.L. Wang, W.Z. Mu, P.G. Jönsson, W.H. Yang. Synergistic effect of the co-pyrolysis of cardboard and polyethylene: A kinetic and thermodynamic study. Energy, 229 (2021), p. 120693. https://doi.org/10.1016/j.energy.2021.120693.

[4] N. Sophonrat, L. Sandstrom, A.C. Johansson, W.H. Yang. Co-pyrolysis of mixed plastics and cellulose: An interaction study by Py-GC×GC/MS. Energ Fuel, 31 (10) (2017), pp. 11078-11090. https://doi.org/10.1021/acs.energyfuels.7b01887.

[5] F. Zhang, M.H. Zeng, R.D. Yappert, J.K. Sun, Y.H. Lee, A.M. LaPointe, B. Peters, M.M. Abu-Omar, S.L. Scott. Polyethylene upcycling to long-chain alkylaromatics by tandem hydrogenolysis/aromatization. Science, 370 (6515) (2020), pp. 437-441. https://doi.org/10.1126/science.abc5441.

[6] B.M. Weckhuysen. Creating value from plastic waste. Science, 370, (6515) (2020), pp. 400-401. https://doi.org/10.1126/science.abe3873.

[7] H. Jeswani, C. Kruger, M. Russ, M. Horlacher, F. Antony, S. Hann, A. Azapagic. Life cycle environmental impacts of chemical recycling via pyrolysis of mixed plastic waste in comparison with mechanical recycling and energy recovery. Sci Total Environ, 769 (2021), p. 144483. https://doi.org/10.1016/j.scitotenv.2020.144483.

[8] Y.M. Wen, S.L. Wang, W.Z. Mu, W.H. Yang, P.G. Jönsson. Pyrolysis performance of peat moss: A simultaneous in-situ thermal analysis and bench-scale experimental study. Fuel, 277 (2020), p. 118173. https://doi.org/10.1016/j.fuel.2020.118173.

[9] Y.M. Wen, Z.Y. Shi, S.L. Wang, W.Z. Mu, P.G. Jönsson, W.H. Yang. Pyrolysis of raw and anaerobically digested organic fractions of municipal solid waste: Kinetics, thermodynamics, and product characterization. Chem Eng J, 415 (2021), p. 129064. https://doi.org/10.1016/j.cej.2021.129064.

[10] L.L. Fan, Y.N. Zhang, S.Y. Liu, N. Zhou, P. Chen, Y.H. Liu, Y.P. Wang, P. Peng, Y.L. Cheng, M. Addy, H.W. Lei, R. Ruan. Ex-situ catalytic upgrading of vapors from microwave-assisted pyrolysis of low-density polyethylene with MgO. Energy Convers Manag, 149 (2017), pp. 432-441. https://doi.org/10.1016/j.enconman.2017.07.039.

[11] Y.Y. Zhang, D.L. Duan, H.W. Lei, E. Villota, R. Ruan. Jet fuel production from waste plastics via catalytic pyrolysis with activated carbons. Appl Energy, 251 (2019), p. 113337. https://doi.org/10.1016/j.apenergy.2019.113337.

[12] L. Quesada, M. Calero, M.A. Martin-Lara, A. Perez, G. Blazquez. Characterization of fuel produced by pyrolysis of plastic film obtained of municipal solid waste. Energy, 186 (2019), p. 115874. https://doi.org/10.1016/j.energy.2019.115874.

[13] H. Akgün, E. Yapıcı, Z. Günkaya, A. Özkan, M. Banar. Utilization of liquid product through pyrolysis of LDPE and C/LDPE as commercial wax. Environ Sci Pollut Res (2021). https://doi.org/10.1007/s11356-021-13999-z.

[14] R.M. Pan, M.F. Martins, G. Debenest. Pyrolysis of waste polyethylene in a semi-batch reactor to produce liquid fuel: Optimization of operating conditions. Energy Convers Manag, 237 (2021), p. 114114. https://doi.org/10.1016/j.enconman.2021.114114.

[15] D.L. Duan, Z.Q. Feng, X.Y. Dong, X.R. Chen, Y.Y. Zhang, K. Wan, Y.P. Wang, Q. Wang, G.S. Xiao, H.F. Liu, R. Ruan. Improving bio-oil quality from low-density polyethylene pyrolysis: Effects of varying activation and pyrolysis parameters. Energy, 232 (2021), p. 121090. https://doi.org/10.1016/j.energy.2021.121090.

[16] E.G. Huo, H.W. Lei, C. Liu, Y.Y. Zhang, L.Y. Xin, Y.F. Zhao, M. Qian, Q.F. Zhang, X.N. Lin, C.X. Wang, W. Mateo, E.M. Villota, R. Ruan. Jet fuel and hydrogen produced from waste plastics catalytic pyrolysis with activated carbon and MgO. Sci Total Environ, 727 (2020), p. 138411. https://doi.org/10.1016/j.scitotenv.2020.138411.

[17] D.H. Zhang, X.N. Lin, Q.F. Zhang, X.J. Ren, W.F. Yu, H.Z. Cai. Catalytic pyrolysis of wood-plastic composite waste over activated carbon catalyst for aromatics production: Effect of preparation process of activated carbon. Energy, 212 (2020), p. 118983. https://doi.org/10.1016/j.energy.2020.118983.

[18] S. Jalalifar, R. Abbassi, V. Garaniya, F. Salehi, S. Papari, K. Hawboldt, V. Strezov. CFD analysis of fast pyrolysis process in a pilot-scale auger reactor. Fuel, 273 (2020), p. 117782. https://doi.org/10.1016/j.fuel.2020.117782.

[19] Singh, V.K. and Kumar, E.A., 2017. Measurement of CO2 adsorption kinetics on activated carbons suitable for gas storage systems. Greenhouse Gases: Science and Technology, 7(1), pp.182-201. https://doi.org/10.1002/ghg.1641

[20] R. Pan, J.V.F. Duque, G. Debenest. Waste plastic thermal pyrolysis analysis by a neural fuzzy model coupled with a genetic algorithm. Waste Biomass Valor, 13 (2022), pp. 135-148. https://doi.org/10.1007/s12649-021-01522-x.

[21] R.M. Pan, J.V.F. Duque, M.F. Martins, G. Debenest. Application of a neural fuzzy model combined with simulated annealing algorithm to predict optimal conditions for polyethylene waste non-isothermal pyrolysis. Heliyon, 6 (11) (2020), p. e05598. https://doi.org/10.1016/j.heliyon.2020.e05598.

[22] R.M. Pan, J.V.F. Duque, G. Debenest. Investigating waste plastic pyrolysis kinetic parameters by genetic algorithm coupled with thermogravimetric analysis. Waste Biomass Valori, 12 (2021), pp. 2623-2637. https://doi.org/10.1007/s12649-020-01181-4.

[23] R. Hasanzadeh, M. Mojaver, T. Azdast, C.B. Park. Polyethylene waste gasification syngas analysis and multi-objective optimization using central composite design for simultaneous minimization of required heat and maximization of exergy efficiency. Energy Convers Manag, 247 (2021), p. 114713. https://doi.org/10.1016/j.enconman.2021.114713.

[24] X.Y. Jie, W.S. Li, D. Slocombe, Y.G. Gao, I. Banerjee, S. Gonzalez-Cortes, B.Z. Yao, H. AlMegren, S. Alshihri, J. Dilworth, J. Thomas, T.C. Xiao, P. Edwards. Microwave-initiated catalytic deconstruction of plastic waste into hydrogen and

high-value carbons. Nat Catal, 3 (11) (2020), pp. 902-912. https://doi.org/10.1038/s41929-020-00518-5.

[25] E. Santos, B. Rijo, F. Lemos, M.A.N.D.A. Lemos. A catalytic reactive distillation approach to high density polyethylene pyrolysis – Part 2 – Middle olefin production. Catal Today (2020). https://doi.org/10.1016/j.cattod.2020.06.014.

[26] W.W. Wang, Y.C. Lu, K.W. Xu, K. Wu, Z.S. Zhang, J.H. Duan. Experimental and simulated study on fluidization characteristics of particle shrinkage in a multi-chamber fluidized bed for biomass fast pyrolysis. Fuel Process Technol, 216 (2021), p. 106799. https://doi.org/10.1016/j.fuproc.2021.106799.

[27] E. Santos, B. Rijo, F. Lemos, M.A.N.D.A. Lemos. A catalytic reactive distillation approach to high density polyethylene pyrolysis – Part 1 – Light olefin production. Chem Eng J, 378 (2019), p. 122077. https://doi.org/10.1016/j.cej.2019.122077.

[28] E. Bagi, H. Baseri. Pyrolysis of Ligustrum vulgare waste and the effects of various operating parameters on bio-oil upgrading. Biomass Convers Biorefin (2021). https://doi.org/10.1007/s13399-021-01374-4.

[29] L.L. Fan, L. Liu, Z.G. Xiao, Z.Y. Su, P. Huang, H.Y. Peng, S. Lv, H.W. Jiang, R. Ruan, P. Chen, W.G. Zhou. Comparative study of continuous-stirred and batch microwave pyrolysis of linear low-density polyethylene in the presence/absence of HZSM-5. Energy, 228 (2021), p. 120612. https://doi.org/10.1016/j.energy.2021.120612.

[30] K. Sun, W.L. Wang, N.J. Themelis, A.C.T. Bourtsalas, Q.X. Huang. Catalytic co-pyrolysis of polycarbonate and polyethylene/polypropylene mixtures: Promotion of oil

deoxygenation and aromatic hydrocarbon formation. Fuel, 285 (2021), p. 119143. https://doi.org/10.1016/j.fuel.2020.119143.

[31] Y.C. Zhang, P. Fu, W.M. Yi, Z.H. Li, Z.Y. Li, S.Q. Wang, Y.J. Li. Species transport and reaction characteristics between gas and solid phases for ex-situ catalytic pyrolysis of biomass. Energy, 225 (2021), p. 120212. https://doi.org/10.1016/j.energy.2021.120212.

[32] F.F. Xu, B. Wang, D. Yang, J.H. Hao, Y.Y. Qiao, Y.Y. Tian. Thermal degradation of typical plastics under high heating rate conditions by TG-FTIR: Pyrolysis behaviors and kinetic analysis. Energy Convers Manag, 171 (2018), pp. 1106-1115. https://doi.org/10.1016/j.enconman.2018.06.047.

[33] C.X. Wang, H.W. Lei, X. Kong, R.G. Zou, M. Qian, Y.F. Zhao, W. Mateo. Catalytic upcycling of waste plastics over nanocellulose derived biochar catalyst for the coupling harvest of hydrogen and liquid fuels. Sci Total Environ, 779 (2021), p. 146463. https://doi.org/10.1016/j.scitotenv.2021.146463.

[34] P. Das, P. Tiwari. Valorization of packaging plastic waste by slow pyrolysis. Resour Conserv Recycl, 128 (2018), pp. 69-77. https://doi.org/10.1016/j.resconrec.2017.09.025.

[35] C.S. Costa, M. Munoz, M.R. Ribeiro, J.M. Silva. H-USY and H-ZSM-5 zeolites as catalysts for HDPE conversion under a hydrogen reductive atmosphere. Sustain Energy Fuels, 5 (4) (2021), pp. 1134-1147. https://doi.org/10.1039/D0SE01584A.

[36] T.M. Ukarde, H.S. Pawar. A Cu doped TiO2 catalyst mediated Catalytic Thermo Liquefaction (CTL) of polyolefinic plastic waste into hydrocarbon oil. Fuel, 285 (2021), p. 119155. https://doi.org/10.1016/j.fuel.2020.119155.

[37] Y.Y. Fan, C. Liu, X.C. Kong, Y. Han, M. Lei, R. Xiao. A new perspective on polyethylene-promoted lignin pyrolysis with mass transfer and radical explanation. Green Energy Environ (2021). https://doi.org/10.1016/j.gee.2021.02.004.

[38] I. Muhammad, G. Manos. Simultaneous pretreatment and catalytic conversion of polyolefins into hydrocarbon fuels over acidic zeolite catalysts. Process Saf Environ, 146 (2021), pp. 702-717. https://doi.org/10.1016/j.psep.2020.12.012.

[39] S. Das, V.V. Goud. RSM-optimised slow pyrolysis of rice husk for bio-oil production and its upgradation. Energy, 225 (2021), p. 120161. https://doi.org/10.1016/j.energy.2021.120161.

[40] M. Qian, H.W. Lei, E. Villota, Y.F. Zhao, E.G. Huo, C.X. Wang, W. Mateo, R.G. Zou. Enhanced production of renewable aromatic hydrocarbons for jet-fuel from softwood biomass and plastic waste using hierarchical ZSM-5 modified with lignin-assisted re-assembly. Energy Convers Manag, 236 (2021), p. 114020. https://doi.org/10.1016/j.enconman.2021.114020.

[41] C.X. Wang, H.W. Lei, R.G. Zou, M. Qian, W. Mateo, X.N. Lin, R. Ruan. Biochar-driven simplification of the compositions of cellulose-pyrolysis-derived biocrude oil coupled with the promotion of hydrogen generation. Bioresour Technol, 334 (2021), p. 125251. https://doi.org/10.1016/j.biortech.2021.125251.

[42] C. Kassargy, S. Awad, G. Burnens, K. Kahine, M. Tazerout. Experimental study of catalytic pyrolysis of polyethylene and polypropylene over USY zeolite and separation to gasoline and diesel-like fuels. J Anal Appl Pyrolysis, 127 (2017), pp. 31-37.

https://doi.org/10.1016/j.jaap.2017.09.005.

[43] S.L. Wong, N. Ngadi, T.A.T. Abdullah, I.M. Inuwa. Conversion of low density polyethylene (LDPE) over ZSM-5 zeolite to liquid fuel. Fuel, 192 (2017), pp. 71-82. https://doi.org/10.1016/j.fuel.2016.12.008.

[44] P. Das, P. Tiwari. The effect of slow pyrolysis on the conversion of packaging waste plastics (PE and PP) into fuel. Waste Manage, 79 (2018), pp. 615-624. https://doi.org/10.1016/j.wasman.2018.08.021.

[45] C.X. Wang, H.W. Lei, M.R.O. Qian, E.G. Huo, Y.F. Zhao, Q.F. Zhang, W. Mateo, X.N. Lin, X. Kong, R.G. Zou, R. Ruan. Application of highly stable biochar catalysts for efficient pyrolysis of plastics: a readily accessible potential solution to a global waste crisis. Sustain Energy Fuels, 4 (9) (2020), pp. 4614-4624. https://doi.org/10.1039/D0SE00652A.

[46] K. Saeaung, N. Phusunti, W. Phetwarotai, S. Assabumrungrat, B. Cheirsilp. Catalytic pyrolysis of petroleum-based and biodegradable plastic waste to obtain high-value chemicals. Waste Manage, 127 (2021), pp. 101-111. https://doi.org/10.1016/j.wasman.2021.04.024.

[47] A.K. Varma, P. Mondal. Pyrolysis of sugarcane bagasse in semi batch reactor: effects of process parameters on product yields and characterization of products. Ind Crop Prod, 95 (2017), pp. 704-717. https://doi.org/10.1016/j.indcrop.2016.11.039.

[48] J.M. Russell, U.R. Gracida-Alvarez, O. Winjobi, D.R. Shonnard. Update to “Effect of temperature and vapor residence time on the micropyrolysis products of waste high

density polyethylene". Ind Eng Chem Res, 59 (2020), pp. 10716-10719. https://doi.org/10.1021/acs.iecr.0c01134.

[49] F.F. Xu, X. Ming, R. Jia, M. Zhao, B. Wang, Y.Y. Qiao, Y.Y. Tian. Effects of operating parameters on products yield and volatiles composition during fast pyrolysis of food waste in the presence of hydrogen. Fuel Process Technol, 210 (2020), p. 106558. https://doi.org/10.1016/j.fuproc.2020.106558.